

Thermal Conductivity of Periclase (MgO) from First Principles

Stephen Stackhouse*

Department of Geological Sciences, University of Michigan, Ann Arbor, Michigan, 48109-1005, USA

Lars Stixrude†

Department of Earth Sciences, University College London, Gower Street, London WC1E 6BT, United Kingdom

Bijaya B. Karki‡

*Department of Computer Science, Louisiana State University, Baton Rouge, Louisiana 70803, USA
and Department of Geology and Geophysics, Louisiana State University, Baton Rouge, Louisiana 70803, USA
(Received 27 August 2009; revised manuscript received 9 March 2010; published 17 May 2010)*

We combine first-principles calculations of forces with the direct nonequilibrium molecular dynamics method to determine the lattice thermal conductivity k of periclase (MgO) up to conditions representative of the Earth's core-mantle boundary (136 GPa, 4100 K). We predict the logarithmic density derivative $a = (\partial \ln k / \partial \ln \rho)_T = 4.6 \pm 1.2$ and that $k = 20 \pm 5 \text{ W m}^{-1} \text{ K}^{-1}$ at the core-mantle boundary, while also finding good agreement with extant experimental data at much lower pressures.

DOI: 10.1103/PhysRevLett.104.208501

PACS numbers: 91.60.Tn, 66.70.-f, 83.10.Rs

Thermal conductivity is central to our understanding of planetary evolution as it sets the time scale of cooling. Thus the thermal evolution of Earth's core and the history of the geomagnetic field are controlled by the conduction of heat into the overlying mantle [1]. The style and efficiency of mantle convection are also strongly influenced by depth variations in the thermal conductivity [2]. Here we focus on periclase (MgO), thought to be a major constituent of Earth's deep mantle [3].

Despite the importance of this basic physical property, the thermal conductivity of dielectrics remains unknown at pressures typical of planetary interiors. Experimental measurements are challenging and have not been attempted above 40 GPa [4]. The predictions of Debye theory are strongly model dependent with estimated values of the isothermal logarithmic density derivative a ranging from 4 to 8 [5–7], leading to uncertainties in the extrapolated value of the thermal conductivity at the base of the mantle of a factor of 5.

MgO periclase, as a wide-gap insulator with a simple structure (B1) and no phase transformations to well above 400 GPa [8], is an ideal system to study the pressure dependence of the lattice thermal conductivity. Although its thermal conductivity is unknown at the conditions of Earth's core-mantle boundary, numerous experimental and theoretical studies have determined thermodynamic properties under such conditions. These show that calculations based on density functional theory in the local density approximation predict properties, such as its equation of state, heat capacity, and elasticity, in good agreement with experimental values [9–11].

We predict the thermal conductivity of periclase by combining density functional theory with the so-called “direct” nonequilibrium molecular dynamics method [12,13]. This method has previously been used in combi-

nation with classical potentials, but not before in combination with *ab initio* molecular dynamics in which the forces are computed quantum mechanically from density functional theory. Classical potentials are unlikely to give accurate predictions at the extreme pressure-temperature conditions of interest here: lattice thermal conductivity is limited by phonon-phonon scattering, which may be very sensitive to the form of the potential. The widely used Green-Kubo relation [14] does not serve our purposes, because in first-principles calculations it is impossible to uniquely decompose the total energy into individual contributions from each atom.

In the direct method, the thermal conductivity is computed as the ratio of an imposed heat flux to the resulting temperature gradient. The heat flux $J(t)$ is imposed by dividing the simulation cell into notional sections of equal width, and exchanging kinetic energy between “hot” and “cold” sections. The temperature gradient dT/dx is computed from the mean temperature of the intervening sections. Once steady state is reached, the lattice thermal conductivity, k , is calculated from Fourier's law:

$$k = - \frac{\langle J(t) \rangle}{\langle dT/dx \rangle}, \quad (1)$$

where the angle brackets indicate time averages. The precision is improved by averaging temperatures in the two symmetrically equivalent sections in the periodic cell. Because the exchange of kinetic energy renders dynamics in the hot and cold sections non-Newtonian, only the linear portion of the temperature gradient is considered in the calculation of the conductivity.

In order to account for the effects of finite system size we follow the method of [15]. The thermal conductivity is related to the phonon mean-free path via kinetic theory

$$k = \frac{1}{3} C_V v l, \quad (2)$$

where C_V is the volumetric specific heat and v the mean sound velocity. The mean-free path

$$l^{-1} = l_{\text{ph}}^{-1} + l_b^{-1} \quad (3)$$

has two contributions from scattering mechanisms that are assumed to act independently: l_{ph} from phonon-phonon scattering and $l_b = 4/L$ from scattering of phonons from the hot and cold sections. L is the length of the simulation cell, and the factor of 4 arises since phonons originating between hot and cold sections will travel on average one quarter of the simulation cell length before encountering the hot or cold sections. A series of simulations at different values of L with computed values of the thermal conductivity k_L yields the following relationship by combining (3) and (2)

$$k_L^{-1} = k_{\infty}^{-1} + \left(\frac{12}{C_V v} \right) L^{-1}. \quad (4)$$

We determine the value of the thermal conductivity in the limit of infinite system size k_{∞} as the intercept of this relationship. We gain additional insight by computing from the slope the mean phonon velocity v , the phonon mean-free path from Eq. (2), and the mean phonon lifetime $\tau = l/v$; for these computations, we adopt the value of C_V from the local density approximation equation of state [10]. A recent study finds close adherence to Eq. (4) with deviations from linearity producing biases in the value of k_{∞} that are small compared to the uncertainty in our simulations [16].

Our simulations are carried out using the density functional code VASP [17], which we modified to perform nonequilibrium molecular dynamics by incorporating the algorithm for kinetic-energy exchange [13]. We use the local density approximation [18] to the exchange-correlation functional and ultrasoft pseudopotentials [19] (electronic configurations: $3s^2$ for Mg and $2s^2 2p^4$ for O). We fix the kinetic-energy cutoff of the plane-wave basis set at 400 eV, and Brillouin zone sampling was restricted to the gamma point. We use a time step of 1.0 fs and the Nosé thermostat [20] to control the mean temperature. Previous work has shown no significant differences between canonical and microcanonical simulations of thermal conductivity [12].

At each volume-temperature condition, we determine the thermal conductivity of periclase for four different simulation cell sizes [$2 \times 2 \times 6$ conventional unit cells (192 atoms), $2 \times 2 \times 8$ (256 atoms), $2 \times 2 \times 12$ (384 atoms), $2 \times 2 \times 16$ (512 atoms)]. Since the phonon mean-free path is a few nanometers even at the high temperatures of interest here, our systems are elongated. The limited cross-sectional area perpendicular to the longer direction is not expected to have a significant effect on results [15]. The simulation cells are divided into sections one atomic layer in width and the hot and cold sections and

those either side of them were excluded in the calculation of the temperature gradient. We equilibrate each simulation with 1 ps of equilibrium molecular dynamics before a further 32 ps of nonequilibrium molecular dynamics, which was long enough for the cumulative average of the calculated lattice thermal conductivity at each cell size to converge to 5%–10% for the largest cells [21]. The first 2 ps of the nonequilibrium molecular dynamics is allowed for steady state to be reached and disregarded in the calculation of thermal conductivity. Uncertainties in the temperature of the sections, heat flux, and lattice thermal conductivity are estimated using the appropriate statistics [22]. The imposed heat flux is controlled by the exchange period t_{ex} : the interval between exchanges of kinetic energy between hot and cold sections. We set t_{ex} such that temperature perturbations are a few hundred kelvins [21]. At the high temperatures of interest, we find that computed values of k are insensitive to the choice of t_{ex} and the magnitude of the temperature gradient: values of k_L differ by less than the statistical uncertainty for values of t_{ex} that differ by a factor of 5 [21].

The variation of the computed thermal conductivity with system size follows closely Eq. (4) (Fig. 1): lattice thermal conductivity increases with simulation cell length, because of the decreasing importance of phonon-boundary scattering [Eq. (3)]. The variation of the thermal conductivity with system size is less than the variation in the thermal conductivity with pressure and temperature over the range studied here. Indeed the raw results show clear trends: k_L increases systematically on compression and cooling for all system sizes.

We see also a systematic variation of the slope of the relationship (4) with pressure-temperature conditions that is caused by an increase in the mean phonon velocity v on compression and cooling (Fig. 1). Our values of the mean phonon velocity are very similar to the Debye velocity

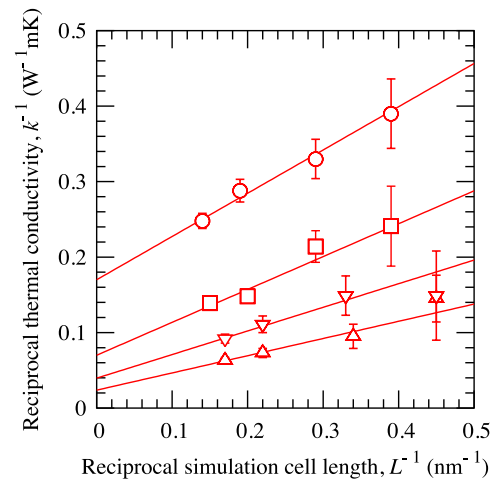


FIG. 1 (color online). Calculated reciprocal thermal conductivities versus reciprocal simulation cell length for each condition studied: (\square) -2 GPa and 1000 K, (\circ) 1 GPa and 2000 K, (\triangle) 149 GPa and 2000 K, and (∇) 161 GPa and 4000 K.

TABLE I. Calculated phonon velocities v , phonon mean-free paths l , and phonon lifetimes τ . Also shown for comparison are the Debye velocities v_D taken from previous work [9].

P (GPa)	T (K)	v (km s $^{-1}$)	v_D (km s $^{-1}$)	l (nm)	τ (ps)
-2	1000	7.0 ± 2.0	6.3	1.6 ± 0.7	0.22 ± 0.11
1	2000	6.0 ± 1.4	5.3	0.8 ± 0.2	0.14 ± 0.05
149	2000	8.6 ± 2.6	8.7	2.4 ± 1.6	0.28 ± 0.20
161	4000	6.4 ± 2.5	8.6	2.0 ± 1.4	0.31 ± 0.25

computed within density functional theory [9] at all pressure-temperature conditions (Table I), consistent with most of the heat being transported by the acoustic modes [23]. Our computed value of the phonon mean-free path and phonon lifetime also increase systematically on compression and cooling. The values that we find for l and τ justify *a posteriori* our chosen system sizes and simulation durations as l is less than the simulation cell size and τ is much shorter than our run durations.

Thermal conductivities in the infinite size limit, determined from linear extrapolation to $L^{-1} = 0$, are listed in Table II. We find that the conductivity increases on compression and cooling due to an increase in the phonon mean-free path. Our values of k_∞ are in excellent agreement with low-pressure experimental measurements (Table II and Fig. 2). Our results also agree well with previous low-pressure simulation studies [24,25], which have used different methods including the Green-Kubo method, and a recent *ab initio* study based on molecular dynamics estimation of phonon lifetimes [26]. The latter depends on the computation of phonon lifetimes via the identification of individual vibrational modes in the Fourier transform of the velocity autocorrelation function, and may be difficult to apply to materials more complex than MgO, which will have several modes with similar frequencies. Our method, in contrast, does not suffer from this limitation, and has been applied to liquids as well as solids [12].

At high pressure, where no previous experiments or simulations exist, our predictions serve as a test of approximate theories of the density dependence of the thermal conductivity (Fig. 2). We find that our results for the variation of k_∞ with density and temperature are well represented by

$$k(\rho, T) = 5.9 \left(\frac{\rho}{3.3} \right)^a \left(\frac{2000}{T} \right), \quad (5)$$

where the best fitting value $a = 4.6 \pm 1.2$ represents an average value over the entire pressure-temperature range of

TABLE II. Calculated lattice thermal conductivities k_∞ and thermal diffusivities $D_\infty = k_\infty / \rho C_V$.

P (GPa)	T (K)	ρ (g cm $^{-3}$)	k_∞ (W m $^{-1}$ K $^{-1}$)	D_∞ (mm 2 s $^{-1}$)
-2	1000	3.464	14 ± 4.6	3.6 ± 1.2
1	2000	3.307	5.9 ± 0.9	1.7 ± 0.2
149	2000	5.192	42 ± 25	6.8 ± 4.0
161	4000	5.111	25 ± 15	4.2 ± 2.5

our study. Our value of a is much lower than in a previous experimental study of MgO, which found $a = 9.9$ [27]. This shows that the assumption that a is constant and equal to the low-pressure value over the range of the Earth's mantle is not justified. Indeed, assuming that $a = 9.9$ over the entire pressure range leads to a computed value of the thermal conductivity at 150 GPa and 2000 K that is 11 times larger than our value. For temperatures much greater than the Debye temperature θ_D ($\theta_D = 950$ K for MgO), Debye theory [5] predicts that

$$a = 3\gamma + 2q - 1/3, \quad (6)$$

where γ is the Grüneisen parameter and q is its logarithmic volume derivative. Thus a should decrease on compression, as both γ and q decrease on compression in MgO [10]. The theory yields values of the conductivity at high pressure that are remarkably consistent with our computed values. The agreement is perhaps somewhat fortuitous as the derivation of Eq. (6) is approximate, for example, in not accounting for the variation of γ among different vibrational modes and in equating the mean phonon velocity with the bulk sound velocity, and is strictly limited to materials with one atom in the unit cell. Using Debye theory and a somewhat different set of assumptions in which the distinction between bulk sound velocity and mean phonon velocity is retained in the derivation of a , another study predicted very different values of k at high pressure that are much lower than ours [6]. The wide disagreement among different applications of Debye the-

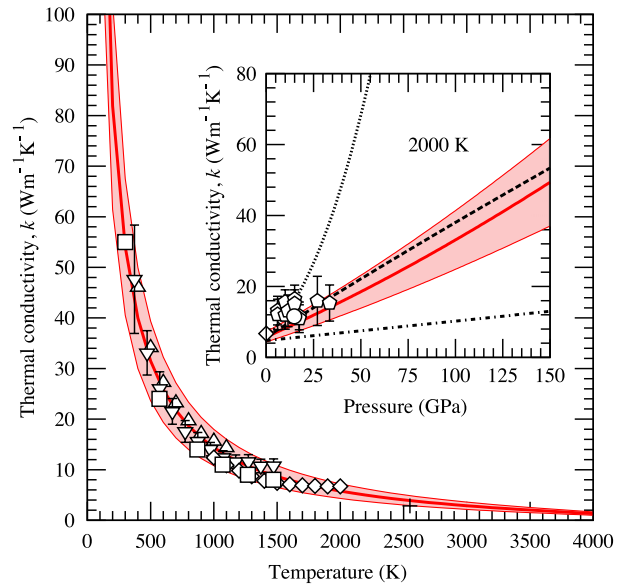


FIG. 2 (color online). Calculated and experimental lattice thermal conductivities of periclase as a function of temperature at $P = 0$ GPa and (inset) as a function of pressure at $T = 2000$ K. Simulation results: This work [Eq. (5)] (solid lines) with 1σ confidence bands (shaded region), (+) [24], (\square) [25], and (\circ) [26]; experimental data: (\triangle) [31], (∇) [27], (\diamond) [32], and (\diamond) [4]; and theory: dotted line [27], dashed line [5], and dot-dashed line [6].

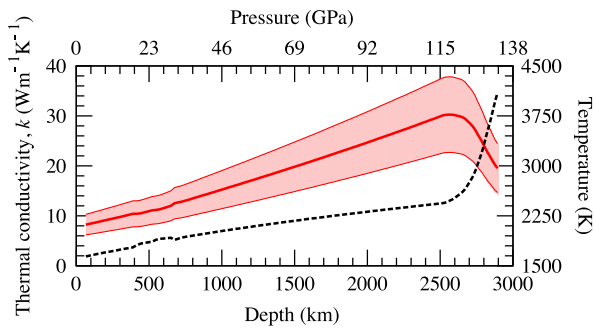


FIG. 3 (color online). Predicted lattice thermal conductivity of MgO from Eq. (5) (solid line) with 1σ confidence bands (shaded region), in Earth's mantle along a model temperature profile [33] (dashed line, right-hand axis).

ory to the prediction of high pressure thermal conductivity [28] emphasizes the importance of *ab initio* predictions.

We predict the thermal conductivity of MgO to increase by a factor of 4 going from a depth of 100 to 2500 km in the lower mantle, before decreasing to a value of $20 \pm 5 \text{ W}^{-1} \text{ K}^{-1}$ at the core-mantle boundary (136 GPa, 4100 K) (Fig. 3). The variation with temperature and pressure is much larger than the typical uncertainties in our calculations and establishes a quantitative basis for any discussion of the heat flow in the deep Earth. We have focused on the lattice thermal conductivity ignoring contributions of defects, including grain boundaries, because these are likely unimportant at the high temperatures of planetary interiors. We have further ignored radiative contributions, as these are known experimentally to be unimportant, due to solid solution of FeO with MgO in Earth's lower mantle [29]. Our value is substantially larger than that typically assumed for the lowermost mantle on the basis of Debye theory ($4\text{--}12 \text{ W m}^{-1} \text{ K}^{-1}$) [6,28,30], and calls into question this widely assumed range of values. Future studies should consider the thermal conductivity of the other phases that are thought to be important in deep planetary mantles, including MgSiO_3 perovskite, to which our *ab initio* method is ideally suited. The thermal conductivity of the orthorhombic perovskite phase will exhibit anisotropy, which is readily explored with our method by performing simulations extended in different crystallographic directions. This allows calculation of the lattice thermal conductivity of materials for which no classical potentials exist or at pressure-temperature regimes in which they are unconstrained.

This research was funded by NSF Grants No. EAR-0635815 and No. EAR-0347204. Portions of this research were conducted with high performance computational resources provided by Louisiana State University. We thank Nico de Koker for helpful discussions.

*s.stackhouse@berkeley.edu

†l.stixrude@ucl.ac.uk

‡karki@csc.lsu.edu

- [1] B. A. Buffett, *Geophys. Res. Lett.* **29**, 1566 (2002).
- [2] J. B. Naliboff and L. H. Kellogg, *Geophys. Res. Lett.* **33**, L12S09 (2006).
- [3] L. Stixrude, R. J. Hemley, and H. K. Mao, *Science* **257**, 1099 (1992).
- [4] A. F. Goncharov, P. Beck, V. V. Struzhkin, B. D. Haugen, and S. D. Jacobsen, *Phys. Earth Planet. Inter.* **174**, 24 (2009).
- [5] R. G. Ross, P. Andersson, B. Sundqvist, and G. Backstrom, *Rep. Prog. Phys.* **47**, 1347 (1984).
- [6] M. Manga and R. Jeanloz, *J. Geophys. Res.* **102**, 2999 (1997).
- [7] A. M. Hofmeister, *Proc. Natl. Acad. Sci. U.S.A.* **104**, 9192 (2007).
- [8] B. B. Karki, L. Stixrude, S. J. Clark, M. C. Warren, G. J. Ackland, and J. Crain, *Am. Mineral.* **82**, 51 (1997).
- [9] B. B. Karki, R. M. Wentzcovitch, S. de Gironcoli, and S. Baroni, *Science* **286**, 1705 (1999).
- [10] N. de Koker and L. Stixrude, *Geophys. J. Int.* **178**, 162 (2009).
- [11] D. Alfè, *Phys. Rev. Lett.* **94**, 235701 (2005).
- [12] F. Müller-Plathe, *J. Chem. Phys.* **106**, 6082 (1997).
- [13] C. Nieto-Draghi and J. B. Avalos, *Mol. Phys.* **101**, 2303 (2003).
- [14] A. J. C. Ladd, B. Moran, and W. G. Hoover, *Phys. Rev. B* **34**, 5058 (1986).
- [15] P. K. Schelling, S. R. Phillpot, and P. Keblinski, *Phys. Rev. B* **65**, 144306 (2002).
- [16] X. W. Zhou, S. Aubry, R. E. Jones, A. Greenstein, and P. K. Schelling, *Phys. Rev. B* **79**, 115201 (2009).
- [17] G. Kresse and J. Furthmüller, *Phys. Rev. B* **54**, 11 169 (1996).
- [18] D. M. Ceperley and B. J. Alder, *Phys. Rev. Lett.* **45**, 566 (1980).
- [19] G. Kresse and J. Hafner, *J. Phys. Condens. Matter* **6**, 8245 (1994).
- [20] S. Nosé, *J. Chem. Phys.* **81**, 511 (1984).
- [21] See supplementary material at <http://link.aps.org/supplemental/10.1103/PhysRevLett.104.208501> for further calculation details.
- [22] H. Flyvbjerg and H. G. Petersen, *J. Chem. Phys.* **91**, 461 (1989).
- [23] G. A. Slack, in *Solid State Physics*, edited by F. Seitz, D. Turnbull, and H. Ehrenreich (Academic, New York, 1979), Vol. 34, pp. 1–70.
- [24] R. E. Cohen, *Rev. High Pres. Sci. Tech.* **7**, 160 (1998).
- [25] P. Shukla, T. Watanabe, J. C. Nino, J. S. Tulenko, and S. R. Phillpot, *J. Nucl. Mater.* **380**, 1 (2008).
- [26] N. de Koker, *Phys. Rev. Lett.* **103**, 125902 (2009).
- [27] T. Katsura, *Phys. Earth Planet. Inter.* **101**, 73 (1997).
- [28] J. M. Brown, *Geophys. Res. Lett.* **13**, 1509 (1986).
- [29] A. F. Goncharov, V. V. Struzhkin, and S. D. Jacobsen, *Science* **312**, 1205 (2006).
- [30] A. M. Hofmeister, *Science* **283**, 1699 (1999).
- [31] H. Kanamori, N. Fujii, and H. Mizutani, *J. Geophys. Res.* **73**, 595 (1968).
- [32] A. M. Hofmeister and D. A. Yuen, *J. Geodyn.* **44**, 186 (2007).
- [33] L. Stixrude, N. de Koker, N. Sun, M. Mookherjee, and B. B. Karki, *Earth Planet. Sci. Lett.* **278**, 226 (2009).